Structural Engineering and Mechanics, Vol. 40, No. 4 (2011) 501-515
DOI: http://dx.doi.org/10.12989/sem.2011.40.4.501

A study on transverse vibration characteristics of a sandwich plate with asymmetrical faces

Namshik Ahn[1a] and Kangsu Lee*[2]

[1]*Department of Architectural Engineering, Free Form Architecture Institute, Sejong University, Seoul 143-747, Korea*
[2]*Korean Register of Shipping, Green and Industrial Technology Center, Daejeon 305-343, Korea*

(Received January 7, 2011, Revised May 4, 2011, Accepted October 12, 2011)

Abstract. Sandwich elements have high flexural rigidity and high strength per density. They also have excellent anti-vibration and anti-noise characteristics. Therefore, they are used for structures of airplanes and high speed ships that must be light, as well as strong. In this paper, the Reissner-Mindlin's plate theory is studied from a Hamilton's principle point of view. This theory is modified to include the influence of shear deformation and rotary inertia, and the equation of motion is derived using energy relationships. The theory is applied to a rectangular sandwich model which has isotropic, asymmetrical faces and an isotropic core. Investigations are conducted for five different plate thicknesses. These plates are identical to the sandwich plates currently used in various structural elements of surface effect ships (SES). The boundary conditions are set to simple supports and fixed supports. The elastic and shear moduli are obtained from the four-point bending tests on the sandwich beams.

Keywords: sandwich; plate; transverse; vibration; asymmetric faces; FRP

1. Introduction

A sandwich structure is one of the most important structural elements used in aircrafts and high speed ships that require light weight and high strength materials. It has high flexural rigidity, high strength per density, high stiffness, and superior anti-vibration and anti-noise characteristics.

Sandwich structures have been studied over a long period of time. During the 1940s and 50s, based on Reissner (Reissner 1945, Reissner 1950)'s plate theory that accounts for shear deformation, a static theory for sandwich plates that considers the shear deformation of the core was introduced and tested for different boundary conditions. In the 50s, Mindlin (1951) published a vibration theory for isotropic, homogeneous plates with rotary inertia and shear deformation. In the 60s, Yu (1966) used Mindlin's theory while analyzing sandwich structures. Ueng (1966) conducted natural frequency analysis by applying the Lagrange multiplier method that meets the boundary conditions for the energy method. In the 70's, several studies using shear deformation theory have been conducted for the free vibration analysis of composite plates (Yang 1966, Whitney 1970, Sun

*Corresponding author, Ph.D., E-mail: leekangsu@gmail.com
[a]Associate Professor, E-mail: nsahn@sejong.ac.kr

1973, Reddy 1979). In the vibration analysis of isotropic moderately thick plates, the shear deformation theory will usually suffice. It is, however, inadequate to model the dynamical behavior of highly orthotropic, composite or sandwich plates using the shear deformation theory, unless appropriate shear correction factors are provided (Liew 1995). Thus many plate theories have been developed to overcome the deficiency of shear deformation theory. From 90s to 2000s, Smeared displacement-based higher-order shear deformation theories were developed first (Lo 1977, Levinson 1980, Kant 1982, Reddy 1984, Pandya 1988, Timarci 1995, Kant 2001). The assumed displacement of these higher-order theories is expressed as a polynomial form of the thickness coordinate. These theories do not account for continuity of the transverse shear stresses and cannot accurately describe the through-the-thickness variation of stresses. A better description can be obtained by layerwise theories (Reddy 1987, Cho 1991, Nosier 1993) that are known to be fairly accurate since they allow a kink in the slope of deflection at each interface between layers. There are several reports on plate vibrations with added point masses, very few reports on plate vibrations with distributed mass loading can be found in the literature (Kim 2007, Alibeiglooa 2008). In the other hand, the free vibration of a simply supported laminated composite plate with distributed patch mass is emphasized (Wong 2002). Rastgaar *et al.* (2006) also presented natural frequencies of laminated composite plates using third-order shear deformation theory. Singh *et al*. (2001) presented natural frequencies of composite plates with random material properties using higher-order shear deformation theory (including rotatory inertia effect). In Korea, using the Rayleigh-Ritz method with a modified plate theory that accounts for shear deformation and the coating effect, a vibration analysis was conducted on sandwich structures that consist of an expanded foam core and FRP symmetric faces. Considering that the structure had very thin, high density faces, that study ignored rotary inertia; the thickness ratio of the face to the core was between 1/70 and 1/100 (Seyed 2009, Afzal 2008, Xin 2008). However, the face to core thickness ratio of an actual ship is much higher than this; it ranges from 1/15 to 1/10. Therefore, its influence has to be considered.

In this study, accounting for shear deflection and rotary inertia of the cross-section due to rotational deflection, a plate theory is derived from Hamilton's principle. This theory is applied to a rectangular sandwich plate model with isotropic and asymmetric faces and core. In addition, a natural frequency analysis is conducted comparing the equation of motion and the Rayleigh-Ritz method. The result is also compared with cases that consider the shear deformation alone. Additional comparison is made between cases that take into account the core density and cases that do not. An investigation is conducted on the influence of the thickness of the core and the faces on the natural frequency.

Five FRP sandwich plate models, which would constitute the upper structure of a surface effect ship (SES), are used in this study. Simple supports are applied as the boundary conditions to this model. Material properties, such as bending and shear moduli of elasticity, are determined from the bending-shear test which is conducted in accordance with "the application manual of the FRP ship structure" of the Korean Register of Shipping.

2. Plate theory

2.1 Hamilton's principle

Dynamic effects are ignored in the principle of minimum potential energy which is often used in

static analysis. The assumptions behind this principle are as follows :
- The mass of the structure is ignored.
- The load is applied to the structure so slowly that the inertial force is zero.

Hamilton's principle expanded this theory to the field of dynamics. By substituting the inertial force acting in the opposite direction for an external force of D'Alembert's principle, a dynamic problem can be solved as a static problem similar to the principle of minimum energy. Following Hamilton's principle, the Euler-Lagrange equation, which describes the force equilibrium, i.e. the equation of motion of the system, is derived from the 1st order variation of the energy relationship.

2.2 Shear deformation and rotary inertia

The plate theory takes into account vertical deformation alone, and it is applicable to plates that are very thin for the area. However, if the thickness is significant compared to the other dimensions, the accuracy of the plate theory would deteriorate. Mindlin considered the rotational deflection of a thick plate and expanded the plate theory to account for shear deformation and rotary inertia. When the rotational deflection is combined with the vertical deformation due to pure bending, the normal to the neutral axis of the plate's cross-section fails to be perpendicular to the axis. Therefore, shear deformation and rotary inertia have to be taken into account along with the inertia in the vertical plane. The assumptions related to this are as follows:
- The plate is isotropic and homogeneous.
- The plate's free surface is the plane $z = \pm h/2$
- $\sigma_z = 0$ (plane stress is considered)
- The cross-section perpendicular to the mid plane of the plate remains straight even after deformation.

3. Vibration theory of the sandwich plate

The bending strain energy of the top and bottom faces, the shear strain energy of the core, and the kinetic energy of the whole structure are applied as the sandwich plate model to the Mindlin's plate theory. In this case, the shear coefficient is defined to be a constant determined based on the

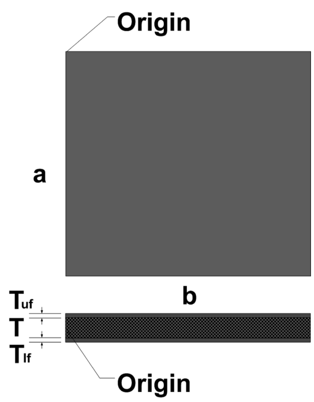

Fig. 1 Analysis model of an asymmetric sandwich plate

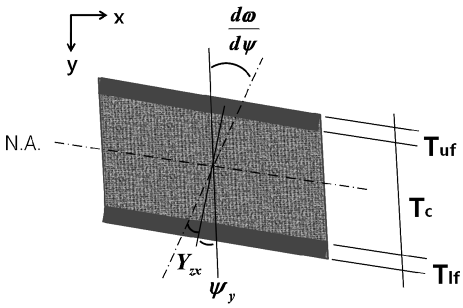

Fig. 2 The *Z-X* plane cross-section of the sandwich plate

geometry of the cross-section, i.e., the width, the thickness of the faces and the core, and the Poisson's ratio. The shear coefficient of a sandwich plate is almost 1 because the core, which has a lower density and strength compared to the faces, hardly resists the bending of the faces. The relationship between the strain, the deformation, and the stress in Mindlin's plate theory is applied to each face and the core. The coordinate system and the analysis model are shown in (Fig. 1).

3.1 Assumptions

The assumptions in the vibration theory of a sandwich plate are as follows:

- The faces and the core are perfectly attached to each other.
- The faces and the core are isotropic. The core is an anti-plane which has a constant shear force regardless of the distance from the center axis.
- The rigidity of the core in the *X-Y* plane is ignored as it is much smaller than that of the faces.
- The *Z* direction stresses of the faces and the core are ignored.
- The shear deformation of the faces is ignored.

In other words, the sandwich plate used in this analysis is assumed to exhibit bending deformation of the faces and shear deformation of the core. The deformed cross-section of the sandwich plate due to deflection is illustrated in (Fig. 2).

3.2 Equation of motion

Considering the vertical inertia and the rotary inertia, the kinetic energy of the faces and the core of an isotropic, homogeneous plate can be given as

$$T = \frac{1}{2}\iint_R \int_{-t_{uf}-t_{uc}}^{t_{lf}+t_{lc}} \rho \dot{u}_i \dot{u}_i dz dA \qquad (i = x, y, z)$$

$$= \frac{1}{2}\iint_R \int_{-t_{uf}-t_{uc}}^{t_{lf}+t_{lc}} \rho \left[z^2 \left(\frac{\partial \psi_x}{\partial t}\right)^2 + z^2 \left(\frac{\partial \psi_y}{\partial t}\right)^2 + \left(\frac{\partial w}{\partial t}\right)^2 \right] dz dA \tag{1}$$

As the top face, core, and the bottom face may have different densities, depending on their thicknesses, (Eq. (1)) is modified for the sandwich plate as

$$T = \frac{1}{2}[\rho_{uf}I_{uf} + \rho_c I_c + \rho_{lf}I_{lf}]\iint_R \left\{\left(\frac{\partial \psi_x}{\partial t}\right)^2 + \left(\frac{\partial \psi_y}{\partial t}\right)^2\right\} dA + \frac{1}{2}[\rho_{uf}t_{uf} + \rho_c t_c + \rho_{lf}t_{lf}]\iint_R \left(\frac{\partial w}{\partial t}\right)^2 dA \quad (2)$$

where, I_{uf}, I_c, and I_{lf} are the second moments of inertia of the top face, the core, and the bottom face, respectively.

The strain energy equation of the plate, ignoring the stress along the Z-direction, is

$$U = \frac{1}{2}\iint_R \int_{-h/2}^{h/2} (\sigma_{xx}\varepsilon_{xx} + \sigma_{yy}\varepsilon_{yy} + 2\sigma_{xy}\varepsilon_{xy} + 2\sigma_{yz}\varepsilon_{yz} + 2\sigma_{zx}\varepsilon_{zx})dzdA$$

Here, the strains due to the plane stress, ε_{xy}, ε_{xx}, and ε_{yy}, are all zeros. Therefore, the shear strain alone is accounted for in the shear strain energy of the core.

$$U_c = \frac{1}{2}\iint_R \int_{-t_{uc}}^{t_{lc}} (2\sigma_{yz}\varepsilon_{yz} + 2\sigma_{zx}\varepsilon_{zx})dzdA$$

$$= \frac{1}{2}kt_c G_c \iint_R \left\{\left(\frac{\partial w}{\partial y} - \psi_y\right)^2 + \left(\frac{\partial w}{\partial x} - \psi_x\right)^2\right\} dA \quad (3)$$

The bending strain energy of the face is given as

$$U_f = U_{lf} + U_{uf}$$

For the faces, only the plane stress is considered and σ_z, γ_{xz}, and γ_{yz} are all zeroes in the equation for the strain energy, U. Therefore, the bending strain energies of the top and bottom faces are

$$U_{uf} = \frac{1}{2}\iint_R \left\{\frac{E}{1-\nu^2}I_{uf}\left[\left(\frac{\partial \psi_x}{\partial x}\right)^2 + \left(\frac{\partial \psi_y}{\partial y}\right)^2 + 2\nu\left(\frac{\partial \psi_x}{\partial x}\frac{\partial \psi_y}{\partial y}\right)\right] + \left(\frac{E}{2(1+\nu)}\right)I_{uf}\left(\frac{\partial \psi_x}{\partial y}\frac{\partial \psi_y}{\partial x}\right)^2\right\} dzdA \quad (4)$$

$$U_{lf} = \frac{1}{2}\iint_R \left\{\frac{E}{1-\nu^2}I_{lf}\left[\left(\frac{\partial \psi_x}{\partial x}\right)^2 + \left(\frac{\partial \psi_y}{\partial y}\right)^2 + 2\nu\left(\frac{\partial \psi_x}{\partial x}\frac{\partial \psi_y}{\partial y}\right)\right] + \left(\frac{E}{2(1+\nu)}\right)I_{lf}\left(\frac{\partial \psi_x}{\partial y}\frac{\partial \psi_y}{\partial x}\right)^2\right\} dzdA \quad (5)$$

The total bending strain energy of the face U_f is

$$U_f = \frac{1}{2}\iint_R \left\{\frac{E}{1-\nu^2}(I_{uf} + I_{lf})\left[\left(\frac{\partial \psi_x}{\partial x}\right)^2 + \left(\frac{\partial \psi_y}{\partial y}\right)^2 + 2\nu\left(\frac{\partial \psi_x}{\partial x}\frac{\partial \psi_y}{\partial y}\right)\right]\right.$$
$$\left. + \left(\frac{E}{2(1+\nu)}\right)(I_{uf} + I_{lf})\left(\frac{\partial \psi_x}{\partial y}\frac{\partial \psi_y}{\partial x}\right)^2\right\} dzdA \quad (6)$$

Where, I_{uf} and I_{lf} are the second moments of inertia of the top and bottom faces, respectively, with respect to the centroid axis.

3.3 Application of the Rayleigh-Ritz method

In order to use the Rayleigh-Ritz method, shape functions w, ψ_x, and ψ_y are defined as

$$w(x,y,t)=\sum_{i=1}^{\infty}\sum_{j=1}^{\infty}a_{mn}\sin\frac{m\pi x}{a}\sin\frac{n\pi y}{b}\sin\omega t \tag{7}$$

$$\psi_x(x,y,t)=\sum_{i=1}^{\infty}\sum_{j=1}^{\infty}b_{mn}\cos\frac{m\pi x}{a}\sin\frac{n\pi y}{b}\sin\omega t \tag{8}$$

$$\varphi_y(x,y,t)=\sum_{i=1}^{\infty}\sum_{j=1}^{\infty}c_{mn}\sin\frac{m\pi x}{a}\cos\frac{n\pi y}{b}\sin\omega t \tag{9}$$

ψ_x and ψ_y reflect the rotation angle due to the deflection of the plate. Therefore, for an isotropic material, the coefficients b_{mn} and c_{mn} would be the same. Using these shape functions, the kinetic and strain energies of the core and the faces are arranged as

$$T_{\max}=\frac{1}{2}(\rho I)^*\omega^2\frac{ab}{4}\sum_{m=1}^{\infty}\sum_{n=1}^{\infty}2b^2{}_{mn}+\frac{1}{2}(\rho h)^*\omega^2\frac{ab}{4}\sum_{m=1}^{\infty}\sum_{n=1}^{\infty}a^2{}_{mn} \tag{10}$$

$$U_{c,\max}=\frac{1}{2}(khG)^*\frac{ab}{4}\sum_{m=1}^{\infty}\sum_{n=1}^{\infty}\left\{\left(\frac{m\pi}{a}a_{mn}-b_{mn}\right)^2+\left(\frac{n\pi}{b}a_{mn}-b_{mn}\right)^2\right\} \tag{11}$$

$$U_{f,\max}=\frac{1}{2}D^*\sum_{m=1}^{\infty}\sum_{n=1}^{\infty}b^2{}_{mn}\left\{\left(\frac{m\pi}{a}\right)^2+\left(\frac{m\pi}{a}\right)^2+2\nu\frac{mn\pi^2}{ab}\right\}+T^*\sum_{m=1}^{\infty}\sum_{n=1}^{\infty}b^2{}_{mn}\left(\frac{n\pi}{b}+\left(\frac{m\pi}{a}\right)^2\right\}\frac{ab}{4} \tag{12}$$

The condition for a stationary value obtained by differentiating the Lagrangian with respect to the shape function coefficients, a_{mn} and b_{mn}, is

$$\frac{\partial(T-U_c-U_f)}{\partial a_{mn}}=\frac{\partial(T-U_c-U_f)}{\partial b_{mn}}=0$$

Therefore, the natural frequency in the (m, n) mode is calculated as

$$\omega_{mn}=\frac{1}{2}\sqrt{\sum_{i=1}^{3}f_i+\frac{\sqrt{\sum_{i=4}^{16}f_i}}{a^2b^2(\rho h)^*(\rho I)^*}} \tag{13}$$

Where,

$$f_1=2(khG)^*\left\{\frac{(\frac{m\pi}{a})^2+(\frac{n\pi}{b})^2}{(\rho h)^*}+\frac{1}{(\rho I)^*}\right\}$$

$$f_2=\frac{D^*}{(\rho I)^*}\left\{(\frac{m\pi}{a})^2+(\frac{n\pi}{b})^2+\frac{2mn\nu\pi^2}{ab}\right\}$$

$$f_3=\frac{T^*}{(\rho I)^*}(\frac{m\pi}{a}+\frac{n\pi}{b})^2$$

$$f_4 = 4a^4b^4((khG)^*)^2((\rho h)^*)^2$$

$$f_5 = 4a^2b^2D^*(khG)^*\pi^2((\rho h)^*)^2(b^2m^2 + a^2n^2 + 2abmn\nu)$$

$$f_6 = (D^*)^2\pi^4((\rho h)^*)^2(b^2m^2 + a^2n^2)^2$$

$$f_7 = 4(D^*)^2\nu\pi^4((\rho h)^*)^2\{(a^2n^2 + b^2m^2 + abmn\nu)abmn$$

$$f_8 = 16a^3b^3mn((khG)^*)^2\pi^2(\rho h)^*(\rho I)^*$$

$$f_9 = -4D^*(khG)^*\pi^4(\rho h)^*(\rho I)^*(b^2m^2 + a^2n^2)^2$$

$$f_{10} = -8D^*(khG)^*\nu\pi^4(\rho h)^*(\rho I)^*(b^2m^2 + a^2n^2)abmn$$

$$f_{11} = 4((khG)^*)^2\pi^4((\rho I)^*)^2(b^2m^2 + a^2n^2)^2$$

$$f_{12} = 4a^2b^2((khG)^*)^2\pi^2((\rho h)^*)^2T^*(bm + an)^2$$

$$f_{13} = 2D^*\pi^4((\rho h)^*)^2T^*\{(b^2m^2 + a^2n^2)^2 + 2(b^2m^2 + a^2n^2)abmn\}$$

$$f_{14} = 2D^*\nu\pi^4((\rho h)^*)^2T^*(bm + an)^2abmn$$

$$f_{15} = -4(khG)^*\pi^4(\rho h)^*(\rho I)^*T^*(b^2m^2 + a^2n^2)^3$$

$$f_{16} = ((\rho h)^*)^2(T^*)^2\pi^4\{(b^2m^2 + a^2n^2) + 2abmn\}^2$$

From the Rayleigh-Ritz method which can be compared the maximum potential energy and kinetic energy for a system. We can get the fundamental mode frequency and shape. To get higher natural frequencies the approximation function of deflection can be assumed as a series of independent function n^{th} and be applied to the Rayleigh method.

$$W(x) = \sum_{i=1}^{n} c_i\phi_i(x, y)$$

$\phi_i(x, y)$ is linearly independent function. For c_i of any magnitude since the Rayleigh Quotient is to be a stationary value as the following relations.

$$\frac{\partial\omega^2}{\partial c_i} = 0, 1, 2, 3, \ldots$$

The necessary condition for obtaining a non-trivial solution is

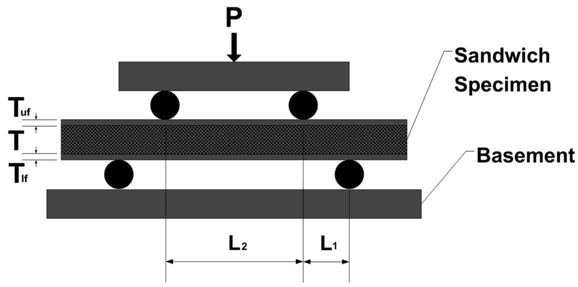

Fig. 3 4-point bending test

$$\left|\alpha_{ij} - \omega^2 \beta_{ij}\right| = 0 \tag{14}$$

Finally, through the Rayleigh-Ritz method, we can basically get the frequency of (i, j) mode from Eq. (14) condition.

4. Structural test and structural properties of sandwich plates

4.1 Bending-shear test

The bending-shear test was conducted according to the FRP structure application manual of the Korean Register of Shipping, and the bending and shear moduli of elasticity were determined. The test setup to measure the second moment of inertia and the shear stress per unit area is illustrated in (Fig. 3). Once the width and the thickness of the specimen are measured, it is supported by the rollers and the load is applied through a crosshead in the middle.

The bending and shear moduli of elasticity are obtained from the test using (Eq. (15) and Eq. (16)), respectively.

$$E = \frac{P}{I\omega(L_1)}\left[-\frac{L_1^3}{12} + CL_1\right] \tag{15}$$

Where, $C = \dfrac{(2L_1+L_2)^3-(L_1+L_2)^3-(L_1)^3}{12(2L_1+L_2)}$ and $\omega(L_1)$ is the deflection.

$$G = \frac{P}{2(t_f+t_c)b}\frac{L_1}{\omega(L_1)} \tag{16}$$

Where, b is the width of the specimen.

4.2 Dimensions and structural properties

The specimens used for the tests are identical to the sandwich plates used in actual ship parts. (Table 1) shows the dimensions of the specimens, and the measured structural properties are listed in (Table 2).

Table 1 Dimensions of the sandwich plates

Plate No.	Application	a (width) [mm]	b (height) [mm]	Thickness [mm]		
				T_{uf}	T_{lf}	T_c
1	BHD	1500	1000	3.5	2.6	49.9
2	Cross Structure	1500	1000	4.6	3.6	39.8
3	Super Structure	1500	1000	3.2	2.8	39.0
4	Wheel House	1500	1000	3.3	2.3	18.9
5	Main Deck	1500	1000	2.5	1.8	20.7

Table 2 Structural properties of the sandwich plates ($\nu = 0.17$)

Plate No.	E_f (bending modulus of inertia) [kg/mm^2]	G_c (shear modulus of inertia) [kg/mm^2]	ρ (density) [kg/mm^3]		
			ρ_{uf} (top face)	ρ_{lf} (bottom face)	ρ_c (core)
1	151.8	3.179	1.446E-6	1.446E-6	7.5E-8
2	266.6	4.342	1.665E-6	1.408E-6	9.0E-8
3	182.4	3.164	2.526E-6	2.526E-6	7.5E-8
4	383.6	3.168	1.665E-6	1.341E-6	7.5E-8
5	343.1	3.325	1.665E-6	1.341E-6	7.5E-8

5. Numerical analysis

5.1 Analytical solution

The natural frequencies calculated using the equation of motion and the Rayleigh-Ritz method are compared. The results indicate that the two methods give very similar frequencies for the (n, n) modes. However, as seen in (Figs. 4-8), the natural frequencies in the (n, $n \pm 2$) modes show discrepancies (1-5 Hz) between the two methods. The figures also show differences in the natural frequencies when the rotary inertia is accounted for and when it is not. The results indicate large

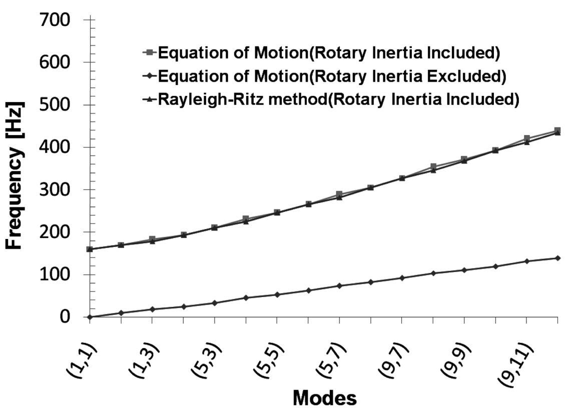

Fig. 4 Natural frequency results for plate 1

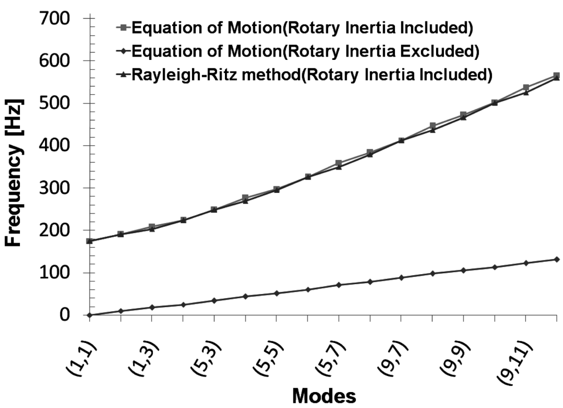

Fig. 5 Natural frequency results for plate 2

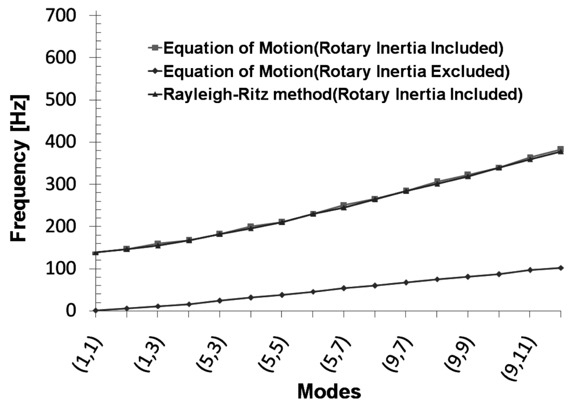

Fig. 6 Natural frequency results for plate 3

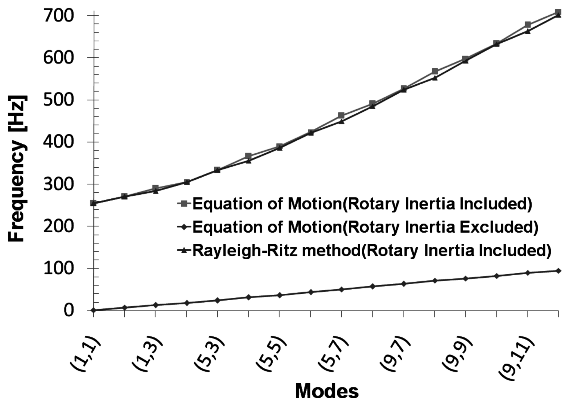

Fig. 7 Natural frequency results for plate 4

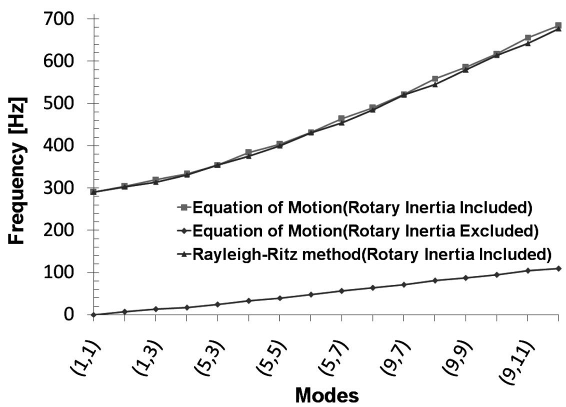

Fig. 8 Natural frequency results for plate 5

Table 3 Dependence of natural frequencies on the core density

Plate No.	Thickness [mm]			Core density included			Core density ignored		
	T_{uf}	T_{lf}	T_c	(ρh^*)	(ρI^*)	(1,1) mode	(ρh^*)	(ρI^*)	(1,1) mode
1	3.5	2.6	49.9	0.12E-4	0.68E-2	156.7	0.88E-5	0.60E-2	167.2
2	4.6	3.6	39.8	0.16E-4	0.64E-2	171.2	0.12E-5	0.58E-2	178.9
3	3.2	2.8	39.0	0.17E-4	0.67E-2	139.4	0.14E-5	0.63E-2	143.6
4	3.3	2.3	18.9	0.99E-4	0.99E-2	252.9	0.85E-5	0.93E-2	260.4
5	2.5	1.8	20.7	0.81E-4	0.86E-2	287.1	0.65E-5	0.80E-2	299.1

differences between the analysis considering shear deformation alone and the analysis where both shear deformation and rotary inertia are accounted for. It is inferred that the differences result from a rotary inertia term, ρI^*, that is two orders of magnitude higher than the vertical inertia term, ρh^*.

Taking into account the density of the core does not alter the location of the centroid, which is the center of the bending moment, but it moves the center of the moment of inertia slightly towards the top face. In addition, for the cases that ignore the core density, both ρh^* and ρI^* decrease, resulting in natural frequencies that are 4-12 Hz higher than those that includes the core density. The differences become larger for higher modes. The results are listed in (Table 3) and shown in (Figs. 9-13).

The influence of altering the thickness of the faces and the core was investigated as follows: The natural frequencies were determined for faces that had 10-190% of the baseline thickness, with 5% increments. The results show higher natural frequencies for thinner faces. In other words, when the thickness of the high-density face was reduced, the influence of the decreased flexural rigidity was lesser than that of the decreased inertia due to the reduction in the mass. In the same way, the natural frequencies for the core that had 10-100% of the baseline thickness were calculated at 1% increments. Comparing the results of varying the core thickness with that of varying face thickness shows that the core thickness change shows lesser difference in ρh^* and much larger differences in ρI^*. In addition, it is observed that, although a reduction in the core thickness results in a smaller shear deformation term $(khG)^*$, the increment in the natural frequency is influenced more by the

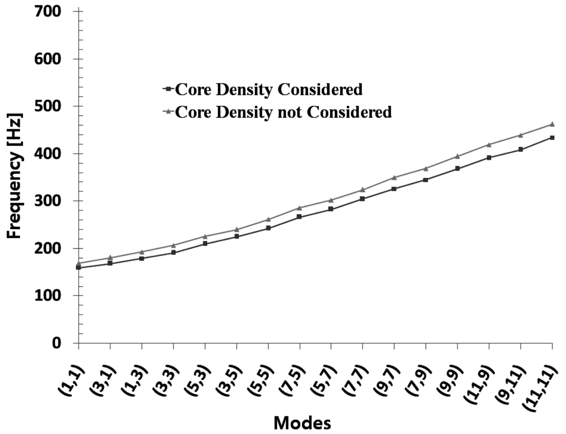

Fig. 9 Difference of natural frequency as core density consideration for plate 1

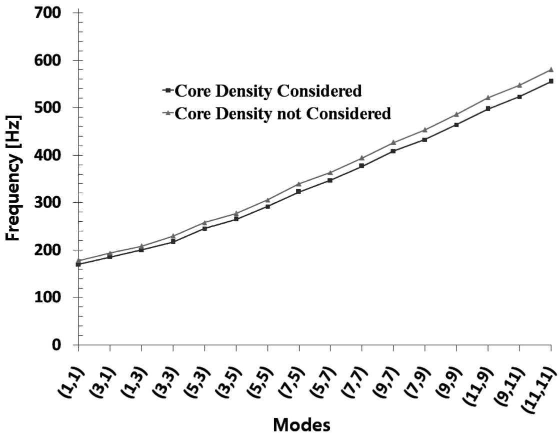

Fig. 10 Difference of natural frequency as core density consideration for plate 2

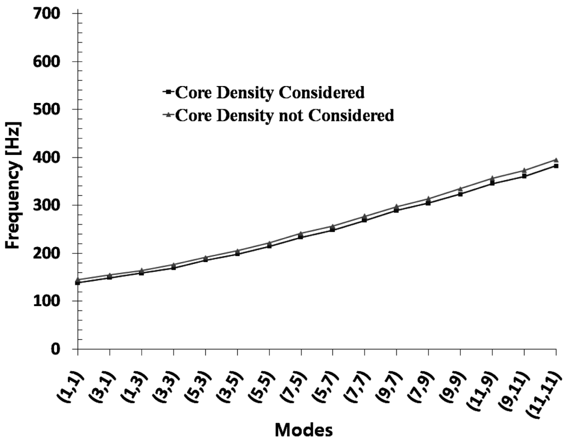

Fig. 11 Difference of natural frequency as core density consideration for plate 3

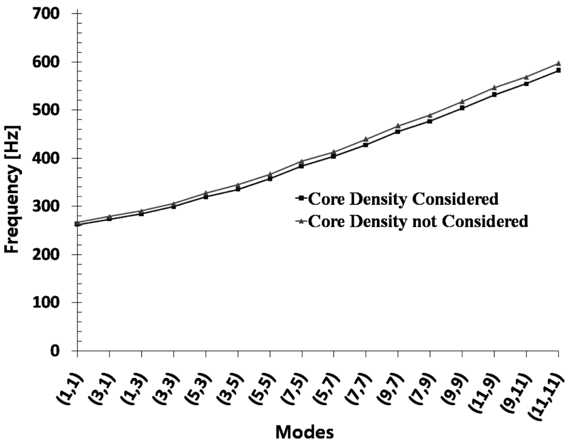

Fig. 12 Difference of natural frequency as core density consideration for plate 4

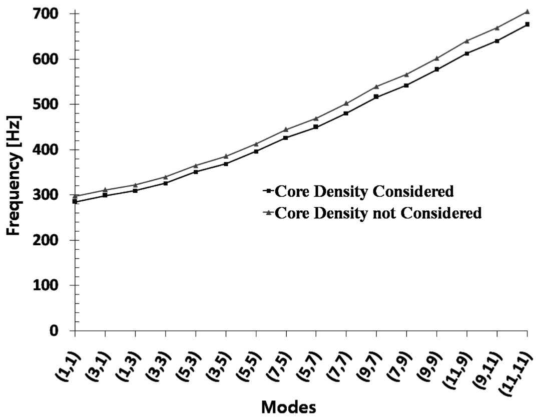

Fig. 13 Difference of natural frequency as core density consideration for plate 5

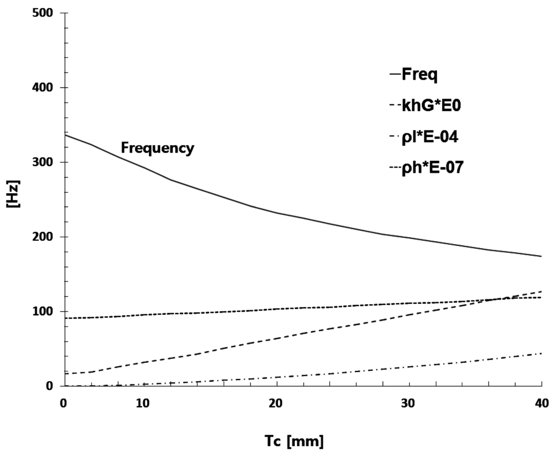

Fig. 14 Variation of natural frequency as core thickness reduction for plate 1

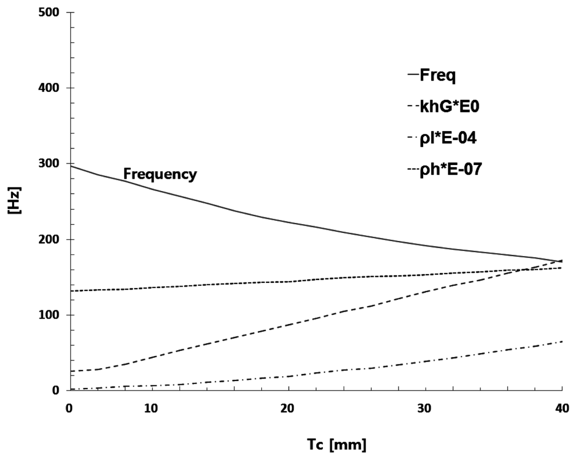

Fig. 15 Variation of natural frequency as core thickness reduction for plate 2

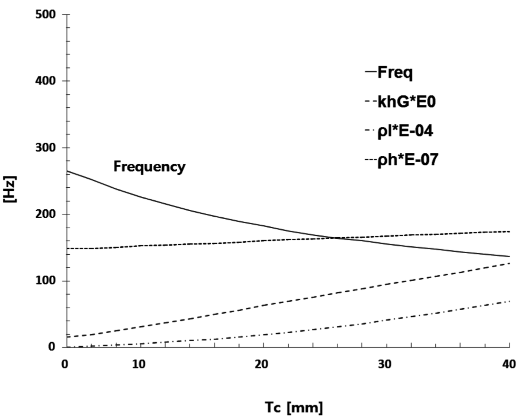

Fig. 16 Variation of natural frequency as core thickness reduction for plate 3

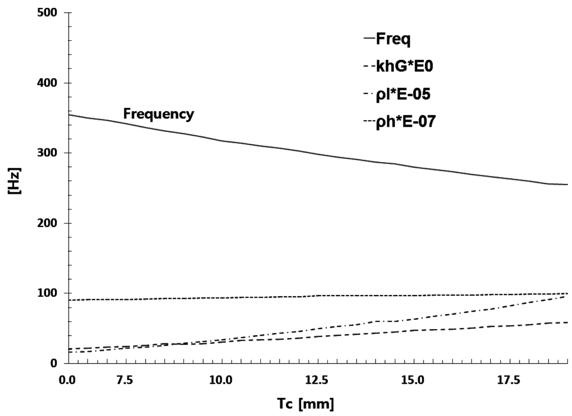

Fig. 17 Variation of natural frequency as core thickness reduction for plate 4

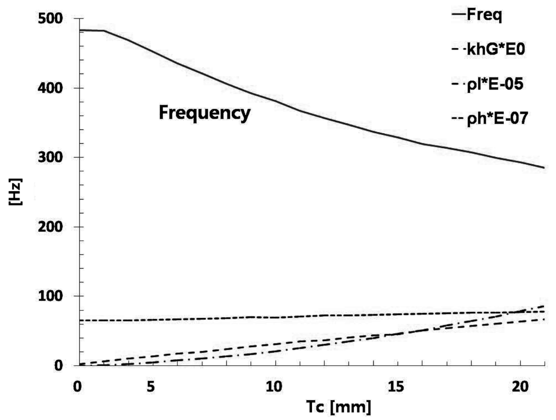

Fig. 18 Variation of natural frequency as core thickness reduction for plate 5

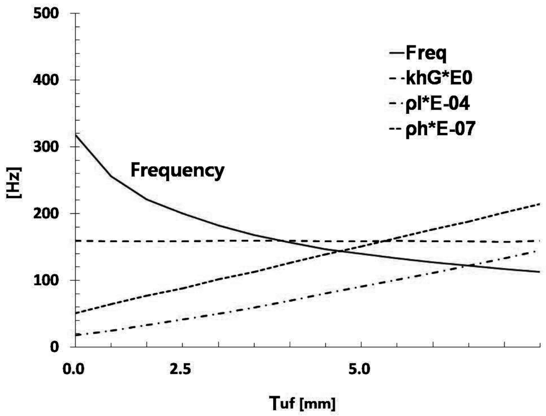

Fig. 19 Variation of natural frequency as face thickness reduction for plate 1

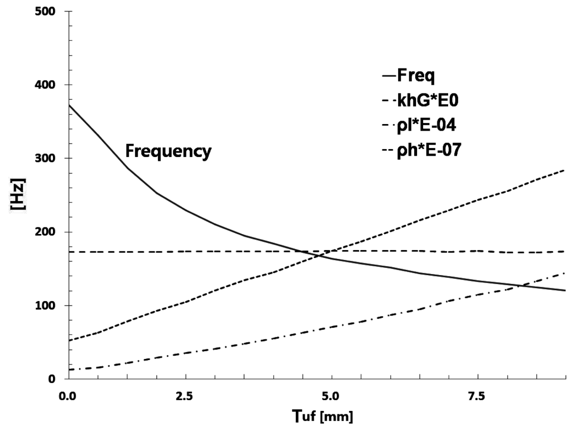

Fig. 20 Variation of natural frequency as face thickness reduction for plate 2

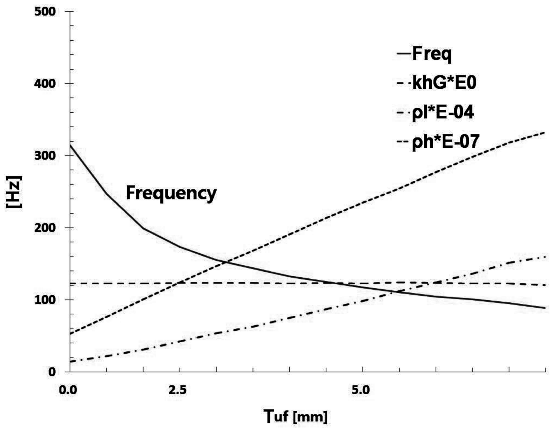

Fig. 21 Variation of natural frequency as face thickness reduction for plate 3

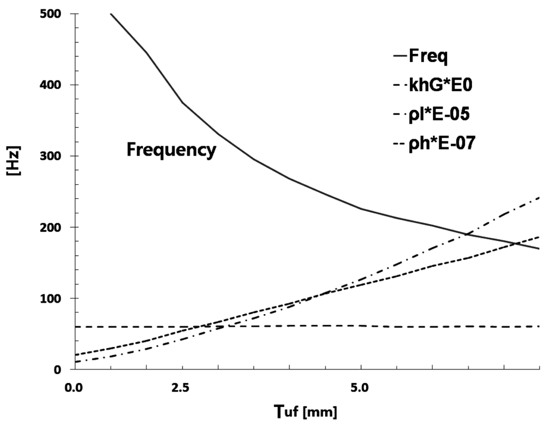

Fig. 22 Variation of natural frequency as face thickness reduction for plate 4

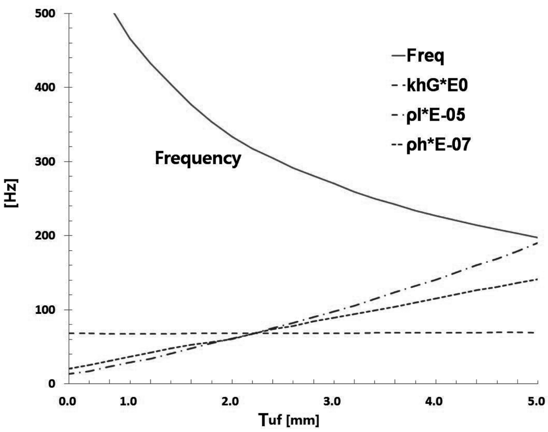

Fig. 23 Variation of natural frequency as face thickness reduction for plate 5

reduction in the moment of inertia. Thus, the main causes for the increased natural frequencies are the reduction in the vertical inertia for thinner faces and the reduction in the rotary inertia for thinner cores.

6. Conclusions

In this study, the vibration characteristics of a rectangular sandwich plate with isotropic, asymmetric faces and core were analyzed. The differences between the natural frequencies obtained with and without rotary inertia were very large. The natural frequency calculated without considering the core density became higher because of the reduced vertical and rotary inertias. The vertical inertia was the primary factor that determined the natural frequency for different thicknesses of the faces, while it was the rotary inertia that mainly affected the natural frequency for different core thicknesses.

In the future, detailed studies should include the damping of the core and the faces and research on anisotropic laminated composite plates should be conducted in detail.

Acknowledgements

This research was supported by the MKE (The Ministry of Knowledge Economy), Korea, under the Convergence-ITRC (Convergence Information Technology Research Center) supervised by the NIPA (National IT Industry Promotion Agency) (NIPA-2011-C6150-1101-0003) and a grant (code# 2009-0087819, 2010-0019373 and 2011-0010300) from the National Research Foundation of Korea (NRF) funded by the Korea government.

References

Alibeiglooa, A., Shakerib, M. and Kari, M.R. (2008), "Free vibration analysis of anti-symmetric laminated rectangular plates with distributed patch mass using third-order shear deformation theory", *J. Oceon. Eng.*, **35**, 183-190.

Cho, K.N., Bert, C.W. and Striz, A.G. (1991), "Free vibrations of laminated rectangular plates analyzed by higher-order individual-layer theory", *J. Sound Vib.*, **145**, 429-442.

Kant, T. (1982), "Numerical analysis of thick plates", *Comm. Meth. Appl. Mech. Eng.*, **31**, 1-18.

Kant, T. and Swaminatha, K. (2001), "Analytical solutions for free vibration of laminated composite and sandwich plates based on a higher-order refined theory", *Comput. Struct*., **53**, 73-85.

Kim, J.S. (2007), "Free vibration of laminated and sandwich plates using enhanced plate theories", *J. Sound Vib.*, **308**, 268-286.

Lee, H.K., Ha, S.K. and Afzal, M. (2008), "Numerical modeling of frp strengthened RC beam-column joints", *Struct. Eng. Mech*., **30**, 247-261

Levinson, M. (1980), "An accurate simple theory of the statics and dynamics of elastic plates", *Mech. Res. Comm.*, **7**, 343-350.

Liew, K.M., Xiang, Y. and Kitipornchai, S. (1995), "Research on thick plate vibration: a literature survey", *J. Sound Vib.*, **180**, 163-176.

Lo, K.H., Christensen, R.M. and Wu, F.M. (1977), "A higher-order theory of plate deformation, part 2: laminated plates", *J. Appl. Mech.*, **44**, 669-676.

Mindlin, R.D. (1951), "Influence of rotary inertia and shear on flexural motions of isotropic, elastic plates", *J. Appl. Mech.*, **18**, 31-38.
Nosier, A., Kapania, R.K. and Reddy, J.N. (1993), "Free vibration analysis of laminated plates using a layer-wise theory", *AIAA J.*, **31**, 2335-2346.
Pandya, B.N. and Kant, T. (1988), "Finite element stress analysis of laminated composite plates using higher order displacement model", *Comput. Sci. Tech.*, **32**, 137-155.
Rastgaar, Agaah M., Mahinfalah, M. and Nakhaie Jazar, G. (2006), "Natural frequencies of laminated composite plates using third-order shear deformation theory", *Concrete Struct*., **72**, 273-279.
Reddy, J.N. (1979), "Free vibration of antisymmetric angle ply laminated plates including transverse shear deformation by the finite element method", *J. Sound Vib.*, **4**, 565-576.
Reddy, J.N. (1984), "A simple higher-order theory for laminated composite plates", *J. Appl. Mech.*, **51**, 745-752.
Reddy, J.N. (1987), "A generalization of two-dimensional theories of laminated plates", *Comm. Numer. Meth. Eng.*, **3**, 173-180.
Reissner, E. (1945), "On bending of elastic plates", *J. Appl. Mech., Trans. ASME*, A-69.
Reissner, E. (1950), "On a variational theorem in elasticity", *J. Math. Phy.*, **29**, 90-95.
Seyed, S.M. and Hamid, R.R. (2009), "Numerical modelling of frp strengthened RC beam-column joints", *Struct. Eng. Mech*., **32**, 649-665.
Singh, B.N., Yadav, D. and Iyengar, N.G.R. (2001), "Natural frequencies of composite plates with random material properties using higher-order shear deformation theory", *Int. J. Mech. Sci.*, **43**, 2193-2214.
Sun, C.T. and Whitney, J.M. (1973), "Theories for the dynamic response of laminated plates", *AIAA J.*, **11**, 178-183.
Timarci, T. and Soldatos, K.P. (1995), "Comparative dynamic studies for symmetric cross-ply circular cylindrical shells on the basis of a unified shear deformable shell theory", *J. Sound Vib.*, **187**, 609-624.
Ueng, C.E.S. (1966), "Natural frequencies of vibration of an all clamped rectangular sandwich panel", *J. Appl. Mech.,* **33**, 683-684.
Whitney, J.M. and Pagano, N.J. (1970), "Shear deformation in heterogeneous anisotropic plates", *J. Appl. Mech.*, **37**, 1031-1036.
Wong, W.O. (2002), "The effects of distributed mass loading on plate vibration behavior", *J. Sound Vib.*, **252**(3), 577-583.
Xin, Z. (2008), "Mechanics feasibility of using Cfrp cables in super long-span cable-stayed bridges", *Struct. Eng. Mech*., **29**, 567-579.
Yang, P.C., Norris, C.H. and Stavsky, Y. (1966), "Elastic wave propagation in heterogeneous plates", *Int. J. Sol. Struct*., **2**, 665-684.
Yu, Y.Y. (1966), "Influence of transverse shear and edges condition on nonlinear vibration and dynamic buckling of homogeneous and sandwich plates", *J. Appl. Mech.*, **33**, 934-936.